Indonesian Journal of Material Research
e-ISSN: 2987-1654
Vol. 2, No. 3, November 2024

Indonesian Journal of MATERIAL RESEARCH

Research Paper

Effectiveness of Modified ZnAl-LDH Developed with POM for Competitive Adsorption of Heavy Metals in Purification Systems

Normah Normah[1*], Melantina Oktriyanti[2], Arini Fousty Badri[2]

[1] *Departement of Chemistry, Universitas Indo Global Mandiri, Palembang 30129, Indonesia*
[2] *Research Centre of Inorganic Materials and Coordination Complexes, Universitas Sriwijaya, Palembang, South Sumatera, 30139, Indonesia*
[*]**Corresponding author**: normah@uigm.ac.id

Abstract
This study investigates the effectiveness of ZnAl-LDH modified with polyoxometalate (POM) as an adsorbent material in the competitive adsorption of heavy metal ions Cr(VI) and Fe(II). The material was synthesized using the co-precipitation method, resulting in ZnAl-LDH@POM with enhanced interlayer spacing, a specific surface area 14 times more significant, and increased surface-active sites. Characterization using XRD, FT-IR, and BET confirmed the successful structural modification and improved adsorption properties. Kinetic studies revealed that adsorption followed a pseudo-second-order kinetic model, achieving maximum efficiency within 50 minutes. Isothermal analysis demonstrated maximum adsorption capacities (Q_{max}) of 92.95 mg/g for Fe(II) and 44.44 mg/g for Cr(VI). These findings highlight the potential of ZnAl-LDH@POM as an effective adsorbent for treating heavy metal-contaminated wastewater.

Keywords
Modified LDH, Adsorption, Heavy Metal, Cr(VI), Fe(II), POM

Received: 19 August 2024, Accepted: 21 November 2024
https://doi.org/10.26554/ijmr.20242347

1. INTRODUCTION

In recent years, rapid industrial development has increased toxic metal ion emissions, severely damaging aquatic ecosystems (dos Santos et al., 2021; Li et al., 2024). Heavy metal ions such as Cr, Pb, Fe, and As, known for their high bioaccumulation properties, have been identified as significant contributors to environmental degradation in water bodies (Babu Poudel et al., 2022; Huang et al., 2022a; Jiang et al., 2024a; Ou et al., 2020). Consequently, effective measures are required to remove and reduce the concentrations of these toxic ions before wastewater is discharged into the environment. Various technologies have been developed for the removal of toxic metals from wastewater, including chemical precipitation, photocatalysis (Ramadhini et al., 2023), adsorption, flocculation, biological treatment, reverse osmosis, and membrane filtration (Liu et al., 2022; Maria Cardinale et al., 2024; Mutahir et al., 2024; Rivers et al., 2024). Among these methods, adsorption stands out due to its high efficiency, simplicity, and relatively low operational costs (Vinsiah et al., 2020; Yuliasari et al., 2022). Factors such as morphological structure, adsorption capacity, specific surface area, dispersibility, chemical/physical stability, and surface charge of the adsorbent play a critical role in determining the efficiency of the adsorption process (Mohadi et al., 2022; Normah et al., 2021; Taher et al., 2024; Zubair et al., 2025).

In this context, developing effective materials for water treatment and removing heavy metal ions has become a primary focus of current research (Zhang et al., 2023). Nanostructured metal oxides and layered double hydroxides (LDH) have emerged as promising adsorbents due to their unique characteristics, including high surface area, abundant active sites, biocompatibility, and chemical and physical stability (Ahmad et al., 2024; Deng et al., 2023; Wibiyan et al., 2024; Zhao et al., 2024). LDHs exhibit structural flexibility, such as tunable composition and ratios of layer-forming elements, variable interlayer anions, and adjustable layer spacing through material modifications (Hanifah and Amri, 2023; Zhao et al., 2023; Kameliya et al., 2023).

Introducing eco-friendly LDH-based materials provides a solution to the limitations of traditional adsorbents. Various LDH materials and their calcined products with diverse morphologies have been successfully synthesized and effectively used to remove a wide range of pollutants from wastewater. In (Tian et al., 2024). However, pristine LDHs often need more structural components that enhance uptake efficiency in adsorption capacity. Various modification strategies have been developed to address these challenges, including anion intercalation, surface modifications, and the formation of composites with other materials (Jiang et al., 2024b). LDHs can be combined with carbon nanostructures, surfactants, iron nanoparticles, or polymers to improve their functional properties (Cao et al., 2023; Huang et al.,

2023; Normah and Lesbani, 2024). These modifications significantly enhance the adsorption capacity of LDHs compared to their unmodified forms, making them more effective and versatile materials for wastewater treatment applications (Altalhi et al., 2024).

Ma et al. (2022) demonstrated the effectiveness of Mg/Al-LDH modification by compositing it with biochar and incorporating egg white as a mediation agent in material formation. This modification increased phosphate adsorption capacity threefold, from 44.17 mg/g to 133.13 mg/g, indicating a monolayer adsorption mechanism with enhanced filament structures on the material surface contributing to improved adsorption performance. LDHs are also known to exhibit various heavy metal adsorption mechanisms, including coordination by interlayer anions, interlayer cation exchange, surface hydroxyl group binding, and hydroxide precipitation resulting from dissolution processes (Huang et al., 2022b; Tian et al., 2024). Fitri et al. (2024) successfully synthesized a Zn-Al/magnetic biochar composite material for malachite green adsorption. This composite demonstrated enhanced structural properties, such as increased specific surface area from 9.621 m^2/g to 99.473 m^2/g, as determined by BET analysis. The adsorption efficiency also doubled compared to pristine LDHs. Another study focused on Abriyanto et al. (2024) the modification of Ca/Al-LDH through intercalation with various anions, such as water, hydroxide, carbonate, and $[\alpha\text{-}SiW_{12}O_{40}]^{4-}$, yielding interlayer spacings of 7.58, 5.04, 7.53, and 4.84 Å, respectively. These results highlight that LDH intercalation significantly influences the structural properties of LDHs, ultimately impacting their adsorption performance.

This study uses a combination of polyoxometalates (POMs) and layered double hydroxides (LDHs) as adsorbents, offering large interlayer spacings through the co-precipitation method. The synthesized LDH materials were characterized using X-ray diffraction (XRD), Fourier-transform infrared spectroscopy (FT-IR), and Brunauer-Emmett-Teller (BET) analysis to determine their structural, functional, and specific surface area properties. Furthermore, the study investigated the material's ability to remove Cr(VI) and Fe(II) ions through comprehensive adsorption kinetics and isothermal behaviour analyses to understand the underlying adsorption mechanisms. The results demonstrated a significant enhancement in heavy metal adsorption capacity with POM-modified LDHs (LDH@POM), establishing them as promising adsorbents for wastewater treatment applications.

2. EXPERIMENTAL SECTION

2.1 Reagents and Materials

All solutions were prepared using deionized water. All chemicals used were of analytical grade without any further purification. Reagents for the synthesis of LDH were obtained from Merck, including zinc nitrate hexahydrate ($Zn(NO_3)_2.6H_2O$, 98.9% purity), aluminium nitrate ($Al(NO_3)_3.9H_2O$, 99% purity), and sodium hydroxide (NaOH, >99% purity). POM was used as a supporting material for the modification, and for the chromium (Cr) adsorption experiments, anhydrous potassium chromate (K_2CrO_4, >99% purity) was dissolved in water to obtain a stock solution with a concentration of 1000 $mg.L^{-1}$. Additionally, 1,5-Diphenylcarbazide ($C_{13}H_{14}N_4O$), acetone (C_6H_6O), sulfuric acid (H_2SO_4, 98% purity), and Iron (II) tetrachloride ($FeCl_2.4H_2O$) and o-phenanthroline monohydrate ($C_{12}H_8N_2$) were obtained from Sigma-Aldrich.

2.2 Synthesis of ZnAl-LDH supported on POM (POM@ZnAl-LDH)

Before synthesizing ZnAl-LDH composited with POM, POM was prepared using a co-precipitation method as outlined in the literature (Chengqian et al., 2023). Once the POM was ready, the synthesis of POM@ZnAl-LDH was conducted via the co-precipitation method (Kameliya et al., 2023). In brief, 22.31 g of $Zn(NO_3)_2.6H_2O$ and 9.38 g of $Al(NO_3)_3.9H_2O$ were dissolved in 100 mL of distilled water and stirred until homogenous. Subsequently, a 1 M NaOH solution was added gradually until the pH reached 10, resulting in the precipitation of ZnAl-LDH. At this stage, 20 g of POM powder was introduced, and the mixture was stirred for 20 minutes. After the formation of the slurry, stirring continued for 62 hours at 70°C. The final product was then dried in an oven at 60°C for 12 hours before ground into powder. The synthesis of unmodified ZnAl-LDH followed the same procedure without adding POM during specific steps.

2.3 Characterization Techniques

The characterization of the crystal structure of the synthesized material was carried out using X-ray diffraction (XRD) with a Rigaku Miniflex-6000 instrument, employing CuKα radiation within the 2θ angle range of 4° to 80°. Functional groups were analyzed via Fourier-transform infrared spectroscopy (FT-IR) within the 4000 to 500 cm^{-1} wavelength range. Nitrogen adsorption-desorption measurements were performed at 77K to determine the specific surface area, pore volume, and pore diameter using a Quantachrome version 3.01 instrument. The adsorption process was analyzed using a UV-Vis spectrophotometer (Biobase BK-UV 1800 PC).

2.4 Adsorption Experiment

The effectiveness of the synthesized POM@ZnAl-LDH composite was evaluated in the adsorption process by calculating the removal efficiency and maximum adsorption capacity for Cr(VI) metal and Fe(II). The adsorption process was carried out using 50 mL of Cr(VI) solution at a concentration of 5 mg L^{-1} and 50 mL of Fe(II) solution at a concentration of 5 mg L^{-1}, with 0.3 g of POM@ZnAl-LDH adsorbent. The adsorption kinetics parameters were analyzed by varying the contact time between the adsorbent and adsorbate at intervals of 0, 5, 10, 20, 25, and up to 180 minutes. The adsorption isotherm parameters were monitored at different temperatures, specifically 30°C, 40°C, 50°C, and 60°C. Throughout the process, the adsorption was performed using a shaker, and after completion, the mixture was separated from the solution by centrifugation. The residual concentration of Cr(VI) was measured using a UV-Vis spectrophotometer at a wavelength of 543 nm after being complexed with 1,5-diphenylcarbazide ($C_{13}H_{14}N_4O$). In comparison, the residual concentration of Fe(II) was measured at a wavelength of 510 nm after being complexed

with 1,10 fenantrolint. The data obtained were used to evaluate the maximum adsorption capacity, along with the kinetics and isotherm characteristics, providing a comprehensive overview of the ZnAl-LDH@POM composite's potential as an adsorbent for removing heavy metal pollutants and organic dyes from aqueous.

3. RESULTS AND DISCUSSION

3.1 Material Characterization

Figure 1 illustrates the X-ray diffraction (XRD) patterns for ZnAl-LDH@POM alongside those for pure ZnAl-LDH and the POM compound. All three materials exhibit pronounced crystallinity, with ZnAl-LDH@POM and ZnAl-LDH showing peaks consistent with the JCPDS standard No. 48-1023 (Lu et al., 2023). Introducing POM compounds results in changes to certain peak angles and intensities in ZnAl-LDH@POM, indicating a blend of structural characteristics from both ZnAl-LDH and the POM compound. Notably, distinct peaks in the XRD pattern of the ZnAl-LDH@POM composite appear around 8.42°, 10°, and within the 20-30° range. Peaks characteristic of ZnAl-LDH at 10.29°, 20.07°, 29.59°, 34.20°, and 60.16° and crystal plane of ZnAl-LDH (003), (006), (012), (110, (113) (Sun et al., 2024) are present in ZnAl-LDH@POM, while new peaks around 8°, 20°, and 25-30° are attributable to the POM compound. This analysis also reveals an increase in interlayer spacing from 8.58 Å(10.19°) in ZNAl-LDH to 10.36 Å(8.53°) in ZnAl-LDH@POM, confirming the successful integration of the POM compound within the layered structure.

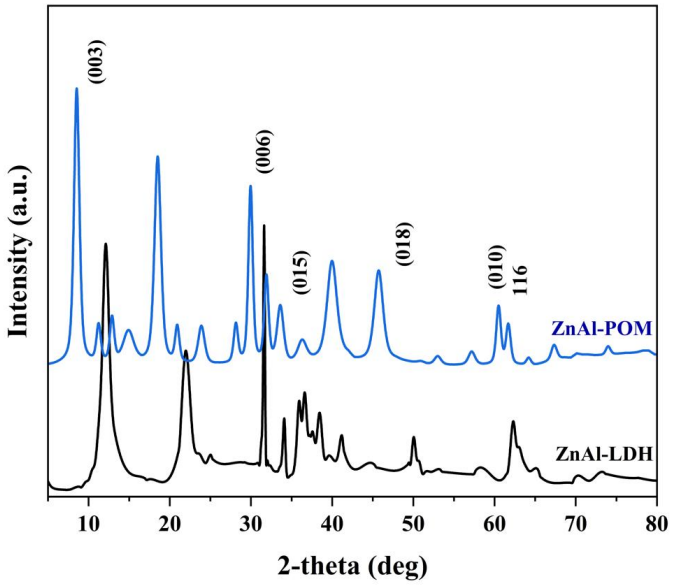

Figure 1. The XRD Patterns of the ZnAl-LDH, POM Compound, and ZnAl-LDH@POM Composite

The Fourier Transform Infrared (FTIR) spectroscopy analysis shown in Figure 2 reveals the chemical bonds and molecular interactions within the ZnAl-LDH@POM composite by measuring infrared absorption at specific wavelengths. The FTIR spectrum of the composite highlights critical peaks corresponding to both ZnAl-LDH and the POM compound. Notably, absorption bands at 1103 cm^{-1} (Si−O−Si) and 894 cm^{-1} (W−O−W) confirm the presence of the POM compound within the composite structure (Liu et al., 2024; Terzi et al., 2023). The peak at 3552 cm^{-1} corresponds to interlayer O−H anions typical of LDH. In comparison, the band at 1631 cm^{-1} suggests H−O−H bending vibrations, likely from water molecules embedded within the LDH layers. A peak at 1379 cm^{-1} indicates the stretching vibrations of various interlayer anions in the composite. Additionally, metal-oxygen bonds are evidenced by absorption peaks at 823 cm^{-1} (Al−O) and 591 cm^{-1} (O−Zn−O), affirming the presence of aluminium and zinc within the LDH structure (Abdelrahman, 2018). Overall, the FTIR spectrum verifies the successful integration of the POM compound into the ZnAl-LDH matrix, preserving characteristic features from both ZnAl-LDH and the POM compound. This confirms the formation of a cohesive composite material.

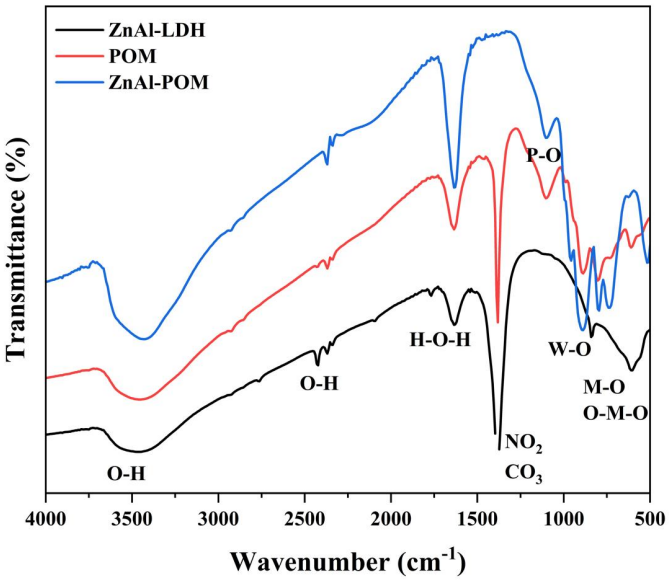

Figure 2. The FT-IR Spectra of the ZnAl-LDH, POM Compound, and ZnAl-LDH@POM Composite

The increase in specific surface area and pore volume suggests (Figure 3) that incorporating POM enhances the materials structural properties, creating more active sites and improving the accessibility of adsorbate molecules. The mesoporous nature of both materials, as indicated by their average pore sizes within the 2–50 nm range, is consistent with type IV isotherms observed in the adsorption-desorption analysis (Lu et al., 2023).

The BET analysis reveals significant differences in the textural properties between ZnAl-LDH and the ZnAl-LDH@POM composite (Table 1). The specific surface area (SBET) of ZnAl-LDH is measured at 1.9685 m^2/g, which indicates a relatively low availability of active sites for adsorption. In contrast, incorporating POM significantly enhances the SBET to 14.042 m^2/g, demonstrating that the modification introduces new structural

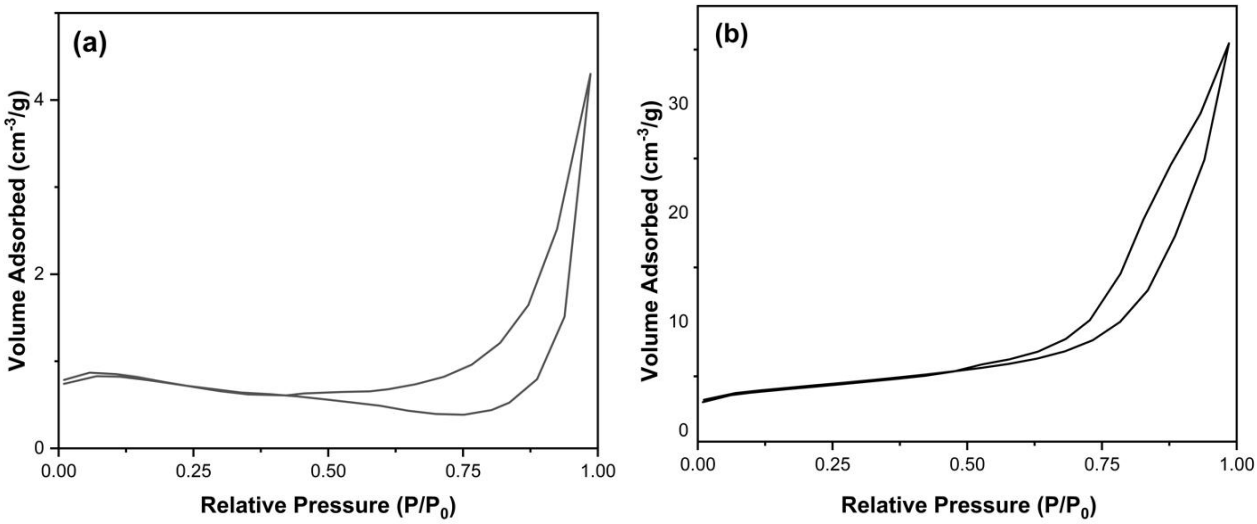

Figure 3. Isotherm of Nitrogen Adsorption-Desorption (a) of ZnAl-LDH and (b) ZnAl-LDH@POM Composite

Table 1. The Characteristics Surface Area Specific Adsorbent of ZnAl-LDH and ZnAl-LDH@POM Composite

Adsorbent	SBET (m^2/g)	Vp (cm^3/g)	Sp (nm)
ZnAl-LDH	1.9685	0.005	13.512
ZnAl-LDH@POM composite	14.042	0.053	15.673

features or improves the accessibility of active sites, thereby increasing the materials adsorption potential. Similarly, the pore volume (Vp) shows a notable increase from 0.005 cm^3/g for ZnAl-LDH to 0.053 cm^3/g for ZnAl-LDH@POM. This enhancement suggests that the modification with POM expands the internal pore structure and provides a higher capacity to accommodate adsorbate molecules (Álvarez et al., 2017).

Furthermore, the pore size (Sp) increases from 13.512 nm to 15.673 nm. The larger pore size in the composite facilitates better accessibility for target molecules, particularly larger ones such as heavy metal ions or organic pollutants. Overall, the improved textural parameters highlight the success of the POM modification in enhancing the adsorption capabilities of ZnAl-LDH. With a higher specific surface area, increased pore volume, and optimal pore size, the ZnAl-LDH@POM composite is expected to exhibit superior adsorption performance compared to the unmodified ZnAl-LDH (Gao et al., 2023; Zheng et al., 2024).

3.2 Adsorption Experimental

3.2.1 Kinetic Adsorption

The adsorption kinetics of Cr(VI) and Fe(II) ions on ZnAl-LDH@POM were evaluated to understand the adsorption mechanism and rate-controlling steps. The data in Figure 4 show that the adsorption process for both ions closely follows the pseudo-second-order kinetic model, as evidenced by the linearity of the plot values (0.996 for Cr(VI) and 0.999 for Fe(II)). For Cr(VI), the pseudo-second-order rate constant (k_2) was determined to be 0.011 g/mg·min, with a slope of 0.0225 and an intercept of 0.0446. In comparison, Fe(II) exhibited a higher rate constant of k_2 = 0.019 g/mg.min, with a slope of 0.0176 and an intercept of 0.0162. These results suggest that the Fe(II) adsorption rate is faster than that of Cr(VI), potentially due to differences in ion size, charge density, or interaction strength with the active sites of ZnAl-LDH@POM.

The pseudo-second-order model indicates that chemisorption is the dominant mechanism involving valence forces or electron sharing between the adsorbate and adsorbent (Zulkarnain et al., 2024). This aligns with the material's mesoporous nature and the availability of active sites, as confirmed by BET analysis. The data further reveal that equilibrium for both Cr(VI) and Fe(II) is achieved within 50 minutes, indicating the efficiency of ZnAl-LDH@POM as an adsorbent. Overall, the higher adsorption rate for Fe(II) and the excellent fit to the pseudo-second-order model demonstrate that ZnAl-LDH@POM has strong potential for the simultaneous removal of Cr(VI) and Fe(II) ions from aqueous solutions (Melak, 2022).

The competitive adsorption behaviour of Fe(II) and Cr(VI) on the ZnAl-LDH@POM surface revealed significant differences influenced by the ionic size, charge, and interaction strength with the material. Fe(II), as a divalent cation with an ionic radius of approximately 0.75 Å, exhibited a faster adsorption rate compared to Cr(VI), which exists predominantly as an anionic species (e.g., $Cr_2O_7^{2-}$ or $HCrO_4^-$) with a larger ionic radius of 7.3 Å. The smaller size and lower hydration radius of Fe(II) facilitated its preferential adsorption onto the active sites of ZnAl-LDH@POM, particularly under conditions where adsorption sites were limited. In contrast, Cr(VI), due to its bulkier oxyanionic structure, encountered steric hindrance and reduced accessibility to ac-

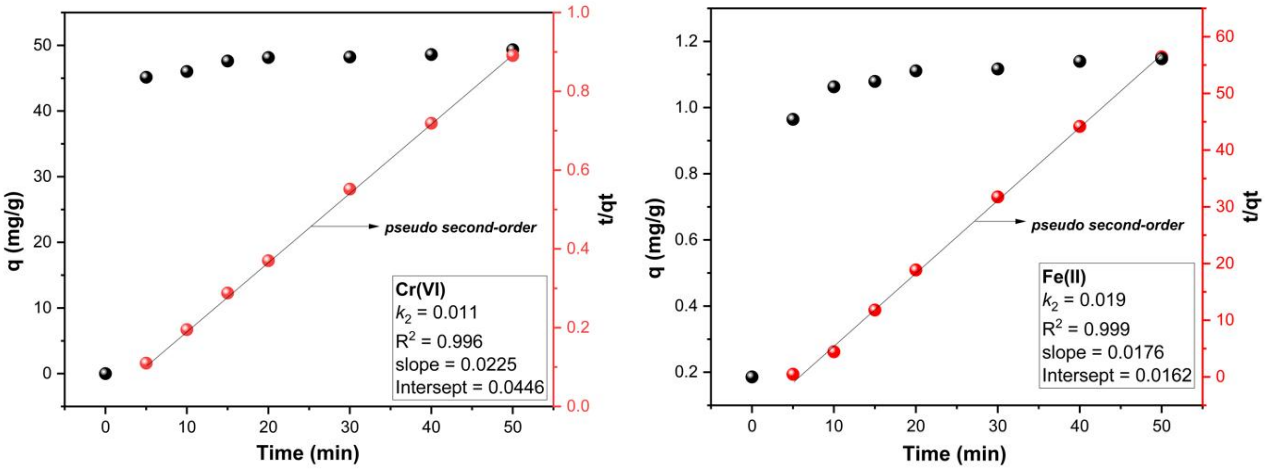

Figure 4. Cr(VI) and Fe (II) Ion Adsorption Contact Time Variation Curve and Kinetic Adsorption of ZnAl-LDH@POM

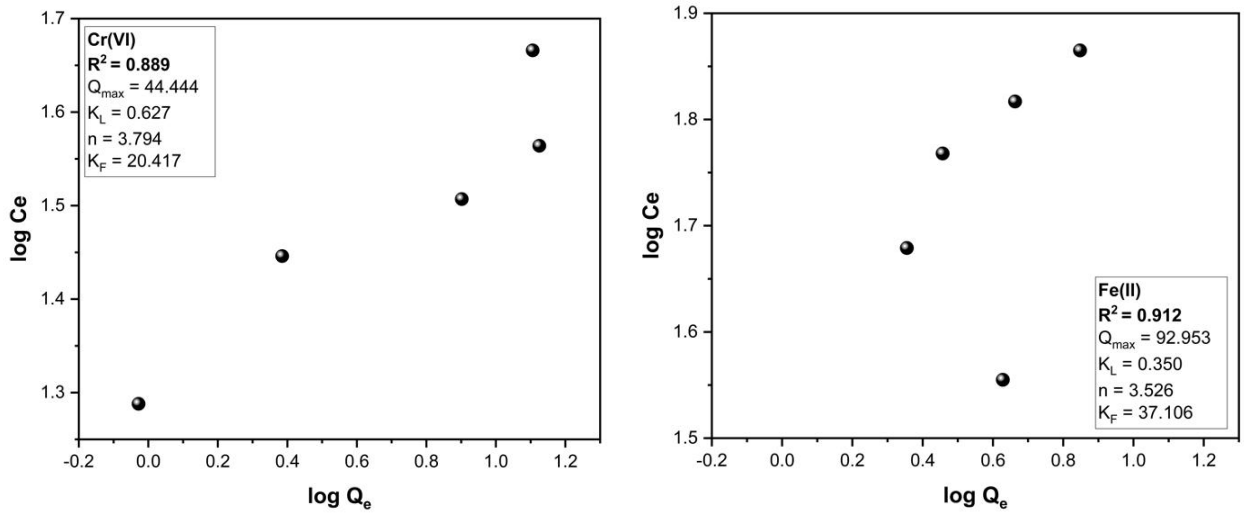

Figure 5. Langmuir Parameters of ZnAl-LDH and ZnAl-LDH@POM Composite

tive sites, especially those already occupied by Fe(II) (Egbosiuba et al., 2021; Melak, 2022). Moreover, the higher oxidation state of Cr(VI) (+6) compared to Fe(II) (+2) influenced the electrostatic interactions with the material's surface. Fe(II) demonstrated stronger interactions with negatively charged or neutral adsorption sites, while weaker interactions and competitive exclusion constrained the adsorption of Cr(VI). These findings underscore the preferential adsorption of Fe(II) in competitive environments, attributed to its smaller ionic size, faster kinetics, and stronger interaction with ZnAl-LDH@POM.

3.2.2 Isotherm Adsorption

The adsorption behaviour of Cr(VI) and Fe(II) ions on ZnAl-LDH@POM was modelled using Langmuir isotherms, as shown in Figure 5. The isotherm parameters provide insights into the adsorption capacity and mechanism. For Cr(VI), the maximum adsorption capacity (Q_{max}) is 44.444 mg/g, with a Langmuir constant (k_L) of 0.627 L/mg, indicating moderate adsorption affinity. The Freundlich constants, n = 3.794 and k_F=20.417, suggest favourable adsorption, as the value of n exceeds 1, confirming a heterogeneous surface interaction (Maria Cardinale et al., 2024). However, the R^2 value for Cr(VI) in the Freundlich model (0.889) is lower than for Fe(II), indicating that Cr(VI) adsorption is less well-fitted to the Freundlich model compared to Fe(II). For Fe(II), the Q_{max} is significantly higher at 92.953 mg/g, with a lower k_L of 0.350 L/mg. The Freundlich constants (n = 3.526 and k_F=37.106) also suggest favourable adsorption with heterogeneous surface characteristics. The higher R^2 value (0.912) indicates that the Freundlich model provides a better fit for Fe(II) adsorption compared to Cr(VI).

The results highlight striking differences in adsorption performance. Fe(II) exhibited a higher adsorption capacity (Q_{max}), attributed to its smaller hydration radius and stronger interactions with the adsorbent surface. In contrast, Cr(VI), predominantly

as oxyanions in aqueous solution, may experience steric hindrance and weaker electrostatic interactions, leading to a lower adsorption capacity. The fit to the Freundlich model suggests that the adsorption of both ions involves multilayer adsorption on a heterogeneous surface, consistent with the mesoporous nature of ZnAl-LDH@POM (Sun et al., 2024). Furthermore, the higher k_F value for Fe(II) reflects stronger adsorption intensity, making the material particularly effective for removing Fe(II) in multicomponent systems (Pei et al., 2024).

4. CONCLUSIONS

This study successfully developed a ZnAl-LDH@POM composite through modification with polyoxometalate (POM), significantly enhancing the adsorption capacity for heavy metal ions Cr(VI) and Fe(II). Characterization revealed improved structural and textural properties, such as a larger specific surface area and increased pore size, which enhanced adsorption efficiency. Kinetic and isothermal studies demonstrated that the adsorption mechanism was dominated by chemisorption and exhibited multilayer characteristics on a heterogeneous surface. ZnAl-LDH@POM exhibited superior performance, particularly in adsorbing Fe(II), making it a strong candidate for wastewater treatment applications.

5. ACKNOWLEDGEMENT

The authors express their gratitude to the Research Center of Inorganic Materials and Complexes at Universitas Sriwijaya for providing laboratory analysis and support and to Universitas Indo Global Mandiri for their invaluable assistance.

REFERENCES

Abdelrahman, E. A. (2018). Synthesis of Zeolite Nanostructures from Waste Aluminum Cans for Efficient Removal of Malachite Green Dye from Aqueous Media. *Journal of Molecular Liquids*, **253**; 72–82

Abriyanto, D., N. Juleanti, N. Normah, and A. Lesbani (2024). Intercalation and Structural Reconstruction of Ca/Al Layered Double Hydroxides. *Indonesian Journal of Material Research*, **2**(2); 51–55

Ahmad, N., A. Wijaya, F. S. Arsyad, I. Royani, and A. Lesbani (2024). Layered Double Hydroxide-Functionalized Humic Acid and Magnetite by Hydrothermal Synthesis for Optimized Adsorption of Malachite Green. *Kuwait Journal of Science*, **51**(2); 100206

Altalhi, A. A., E. A. Mohamed, and N. A. Negm (2024). Recent Advances in Layered Double Hydroxide (LDH)-Based Materials: Fabrication, Modification Strategies, Characterization, Promising Environmental Catalytic Applications, and Prospective Aspects. *Energy Advances*, **3**(9); 2136–2151

Álvarez, M. G., A. Urda, V. Rives, S. R. G. Carrazán, C. Martín, D. Tichit, and I. Marcu (2017). Propane Oxidative Dehydrogenation Over V-Containing Mixed Oxides Derived from Decavanadate-Exchanged ZnAl–Layered Double Hydroxides Prepared by a Sol–Gel Method. *Comptes Rendus. Chimie*, **21**(3–4); 210–220

Babu Poudel, M., M. Shin, and H. Joo Kim (2022). Interface Engineering of MIL-88 Derived MnFe-LDH and $MnFe_2O_3$ on Three-Dimensional Carbon Nanofibers for the Efficient Adsorption of Cr(VI), Pb(II), and As(III) Ions. *Separation and Purification Technology*, **287**; 120463

Cao, J., Z. Feng, H. Liang, X. Lu, and W. Wang (2023). Oriented Self-Assembly of Anisotropic Layered Double Hydroxides (LDHs) with 2D-on-3D Hierarchical Structure. *Chemical Engineering Journal*, **472**; 144872

Chengqian, F., L. Wanbing, D. Yimin, W. Zhiheng, L. Yaqi, C. Ling, L. Bo, Y. Siwen, W. Junlong, D. Xianglong, Z. Yue-Fei, L. Yan, and W. Li (2023). Synthesis of a Novel Hierarchical Pillared Sep@Fe_3O_4/ZnAl-LDH Composite for Effective Anionic Dyes Removal. *Colloids and Surfaces A: Physicochemical and Engineering Aspects*, **663**; 130921

Deng, C., Y. Liu, H. Jian, Y. Liang, M. Wen, J. Shi, and H. Park (2023). Study on the Preparation of Flame Retardant Plywood by Intercalation of Phosphorus and Nitrogen Flame Retardants Modified with Mg/Al-LDH. *Construction and Building Materials*, **374**; 130939

dos Santos, G. E. d. S., P. V. d. S. Lins, L. M. T. d. M. Oliveira, E. O. d. Silva, I. Anastopoulos, A. Erto, D. A. Giannakoudakis, A. R. F. d. Almeida, J. L. d. S. Duarte, and L. Meili (2021). Layered Double Hydroxides/Biochar Composites as Adsorbents for Water Remediation Applications: Recent Trends and Perspectives. *Journal of Cleaner Production*, **284**; 124755

Egbosiuba, T. C., A. S. Abdulkareem, A. S. Kovo, E. A. Afolabi, J. O. Tijani, M. T. Bankole, S. Bo, and W. D. Roos (2021). Adsorption of Cr(VI), Ni(II), Fe(II) and Cd(II) Ions by KIAgNPs Decorated MWCNTs in a Batch and Fixed Bed Process. *Scientific Reports*, **11**(1); 1–20

Fitri, E. S., R. Mohadi, N. R. Palapa, S. A. Rachman, and A. Lesbani (2024). Composite Layered Double Hydroxide Zn-Al/Magnetic Biochar Modified for Highly Effective Malachite Green Adsorption. *Environment and Natural Resources Journal*, **22**(2); 129–144

Gao, D., F. Han, G. I. N. Waterhouse, Y. Li, and L. Zhang (2023). A Highly Efficient Iron Phthalocyanine-Intercalated CuFe-LDH Catalyst for the Selective Oxidation of 5-Hydroxymethylfurfural to 5-Formyl-2-Furanic Acid. *Catalysis Communications*, **173**; 106561

Hanifah, Y. and A. Amri (2023). Preparation of Layered Double Hydroxide-Polyoxometalate Based Composite. *Indonesian Journal of Material Research*, **1**(2); 68–73

Huang, L., L. Wang, C. Wang, and X. Tao (2022a). Effect of Intercalation of Flocculant on Adsorption Properties of ZnMgAl-LDHs. *Inorganic Chemistry Communications*, **135**; 109127

Huang, Y., C. Liu, L. Qin, M. Xie, Z. Xu, and Y. Yu (2023). Efficient Adsorption Capacity of MgFe-Layered Double Hydroxide Loaded on Pomelo Peel Biochar for Cd (II) from Aqueous Solutions: Adsorption Behaviour and Mechanism. *Molecules*, **28**(11); 4538

Huang, Z., C. Xiong, L. Ying, W. Wang, S. Wang, J. Ding, and J. Lu

(2022b). Facile Synthesis of a MOF-Derived Magnetic CoAl-LDH@Chitosan Composite for Pb (II) and Cr (VI) Adsorption. *Chemical Engineering Journal*, **449**; 137722

Jiang, N., B. Du, D. Gao, Z. Chai, C. Liu, and X. Zhu (2024a). Effective As(V) Removal Using in Situ Grown Ti-Based MOFs on ZnAl-LDHs. *Materials Science and Engineering: B*, **303**; 117306

Jiang, Z., M. Wu, P. Gu, W. Huang, C.-P. Yu, Z. Zheng, Y. Wang, N. Yao, and Y. Li (2024b). Layered Double Hydroxide@Zeolite Composite Modified Sponge: A Versatile Biocarrier for Enhancing Nitrogen Removal in Biofilters. *Chemical Engineering Journal*, **481**; 148686

Kameliya, J., A. Verma, P. Dutta, C. Arora, S. Vyas, and R. S. Varma (2023). Layered Double Hydroxide Materials: A Review on Their Preparation, Characterization, and Applications. *Inorganics*, **11**(3); 121

Li, M., X. Chen, J. He, S. Liu, Y. Tang, and X. Wen (2024). Porous NiCo-LDH Microspheres Obtained by Freeze-Drying for Efficient Dye and Cr(VI) Adsorption. *Journal of Alloys and Compounds*, **976**; 173107

Liu, L., T. Zhang, X. Yu, V. Mkandawire, J. Ma, and X. Li (2022). Removal of Fe^{2+} and Mn^{2+} from Polluted Groundwater by Insoluble Humic Acid/Tourmaline Composite Particles. *Materials*, **15**(9); 3130

Liu, X., T. Sun, Y. Sun, A. Manshina, and L. Wang (2024). Polyoxometalate-Based Peroxidase-Like Nanozymes. *Nano Materials Science*, **(In Press)**

Lu, Y., C. Ding, J. Guo, W. Gan, P. Chen, R. Chen, Q. Ling, M. Zhang, P. Wang, and Z. Sun (2023). Cobalt-Doped ZnAl-LDH Nanosheet Arrays as Recyclable Piezo-Catalysts for Effective Activation of Peroxymonosulfate to Degrade Norfloxacin: Non-Radical Pathways and Theoretical Calculation Studies. *Nano Energy*, **112**; 108515

Ma, W., T. T. Lv, J. H. Tang, M. L. Feng, and X. Y. Huang (2022). Highly Efficient Uptake of Cs^+ By Robust Layered Metal-Organic Frameworks with a Distinctive Ion Exchange Mechanism. *JACS Au*, **2**(2); 492–501

Maria Cardinale, A., M. Fortunato, and F. Ardini (2024). NiFe Based Synthetic LDH, Study of Chromate Adsorption Mechanisms. *Results in Surfaces and Interfaces*, **16**; 100242

Melak, F. (2022). Comparative Removal of Cr(VI) and F^- Ions from Water. *Journal of Chemistry*, **1**; 9143182

Mohadi, R., Normah, E. S. Fitri, and N. R. Palapa (2022). Unique Adsorption Properties of Cationic Dyes Malachite Green and Rhodamine-B. *Science and Technology Indonesia*, **7**(1); 115–125

Mutahir, S., S. Akram, M. A. Khan, H. Deng, A. M. Naglah, A. A. Almehizia, M. A. Al-Omar, F. I. Alrayes, and M. S. Refat (2024). Facile Synthesis of Zn/Co LDH for the Removal of Oxytetracycline from Wastewater: Experimental and DFT-Based Analysis. *Chemical Engineering Science*, **283**; 119399

Normah, N. and A. Lesbani (2024). Comparison of LDH-Organic/Inorganic Compound Modified Materials as Adsorbents for Heavy Metal Adsorption: Characteristic Structure and Adsorption Mechanism. *Bulletin of Chemical Reaction Engineering and Catalysis*, **19**(2); 327–339

Normah, N., N. R. Palapa, T. Taher, R. Mohadi, F. S. Arsyad, A. Priambodo, and A. Lesbani (2021). Competitive Removal of Cationic Dye Using NiAl-LDH Modified with Hydrochar. *Ecological Engineering & Environmental Technology*, **22**(4); 124–135

Ou, B., J. Wang, Y. Wu, S. Zhao, and Z. Wang (2020). Efficient Removal of Cr (VI) by Magnetic and Recyclable Calcined CoFe-LDH/g-C_3N_4 via the Synergy of Adsorption and Photocatalysis Under Visible Light. *Chemical Engineering Journal*, **380**; 122600

Pei, Y., W. Cheng, R. Liu, H. Di, Y. Jiang, C. Zheng, and Z. Jiang (2024). Synergistic Effect and Mechanism of nZVI/LDH Composites Adsorption Coupled Reduction of Nitrate in Micro-Polluted Water. *Journal of Hazardous Materials*, **464**; 133023

Ramadhini, T. K., T. E. Agustina, E. Melwita, and M. S. Wijayanti (2023). Photocatalytic Degradation of Heavy Metals Cd, Cu, Fe and Pb Using ZnO-Zeolite Nanocomposite. *Indonesian Journal of Environmental Management and Sustainability*, **7**(4); 147–152

Rivers, G., A. Lion, N. R. E. Putri, G. A. Rance, C. Moloney, V. Taresco, V. C. Crucitti, H. Constantin, M. I. Evangelista Barreiros, L. R. Cantu, C. J. Tuck, F. R. A. J. Rose, R. J. M. Hague, C. J. Roberts, L. Turyanska, R. D. Wildman, and Y. He (2024). Enabling High-Fidelity Personalised Pharmaceutical Tablets Through Multimaterial Inkjet 3D Printing with a Water-Soluble Excipient. *Materials Today Advances*, **22**; 2–8

Sun, S., Y. Zhang, Q. Gao, N. Zhang, P. A. Hu, and W. Feng (2024). ZnAl-LDH Film for Self-Powered Ultraviolet Photodetection. *Nano Materials Science*, **(In Press)**

Taher, T., Z. Yu, E. K. A. Melati, A. Munandar, R. Aflaha, K. Triyana, Y. G. Wibowo, K. Khairurrijal, A. Lesbani, and A. Rianjanu (2024). Enabling Dual-Functionality Material for Effective Anionic and Cationic Dye Removal by Using Nb2O5/MgAl-LDH Nanocomposites. *Journal of Hazardous Materials Letters*, **5**; 100103

Terzi, C. M., E. H. dos Santos, C. Carvalho, V. Prevot, F. Wypych, C. Forano, and S. Nakagaki (2023). MgAl and ZnAl Layered Double Hydroxides Modified with Molybdate and Tungstate Anions as Catalysts for Oxidation of Cyclohexane. *Catalysis Today*, **422**; 114221

Tian, H., H. Yang, Z. Mo, W. Guo, L. Xu, and B. Liu (2024). Removal of Cr(VI) from Electroplating Wastewater by CoNi-LDH@NHCS Electrode and Its Electrocatalytic Ammonia Production. *Journal of Water Process Engineering*, **68**; 106471

Vinsiah, R., R. Mohadi, and A. Lesbani (2020). Performance of Graphite for Congo Red and Direct Orange Adsorption. *Indonesian Journal of Environmental Management and Sustainability*, **4**(4); 125–132

Wibiyan, S., I. Royani, and A. Lesbani (2024). Selective Adsorption of Cationic and Anionic Dyes Using Ni/Al Layered Double Hydroxide Modified with *Eucheuma cottonii*. *Indonesian Journal of Material Research*, **2**(1); 1–6

Yuliasari, N., A. F. Badri, A. Wijaya, P. M. S. B. N. Siregar, M. Amri, R. Mohadi, and A. Lesbani (2022). Modification of Mg/Al-LDH Intercalated Metal Oxide (Mg/Al-Ni) to Improve the Perfor-

mance of Methyl Orange and Methyl Red Dyes Adsorption Process. *Science and Technology Indonesia*, **7**(3); 275–283

Zhang, C., Y. Li, T. Wang, S. Xu, H. Ma, L. Fang, Y. Que, and Y. Chen (2023). Multi-Scale Evaluation of Sodium Dodecyl Sulfate Intercalated LDHs on the Ageing Resistance of SBS Modified Bitumen. *Construction and Building Materials*, **406**; 133369

Zhao, X., H. Jiang, Y. Xiao, and M. Zhong (2024). Synthesis of Polyoxometalate-Pillared Zn-Cr Layered Double Hydroxides for Photocatalytic CO_2 Reduction and H_2O Oxidation. *Nanoscale Advances*, **6**(4); 1241–1245

Zhao, X. J., S. M. Xu, P. Yin, J. Y. Guo, W. Zhang, Y. Jie, and H. Yan (2023). Theoretical Study on the Mechanism of Super-Stable Mineralization of LDHs in Soil Remediation. *Chemical Engineering Journal*, **451**; 138500

Zheng, J., C. Fan, X. Li, Q. Yang, D. Wang, A. Duan, and S. Pan (2024). Efficient Mineralisation and Disinfection of Neonicotinoid Pesticides with Unique ZnAl-LDH Intercalation Structure and Synergistic Effect of Cu2O Crystalline Surface. *Colloids and Surfaces A: Physicochemical and Engineering Aspects*, **687**; 133507

Zubair, Y. O., S. Fuchida, K. Oyama, and C. Tokoro (2025). Morphologically Controlled Synthesis of MgFe-LDH Using MgO and Succinic Acid for Enhanced Arsenic Adsorption: Kinetics, Equilibrium, and Mechanism Studies. *Journal of Environmental Sciences*, **148**; 637–649

Zulkarnain, Y. M., E. Melwita, and R. Mohadi (2024). The Effects of Hydrothermal Temperatures on ZnO-Bentonite Composite Synthesis on Adsorption and Photodegradation of Methylene Blue Dye. *Science and Technology Indonesia*, **9**(4); 1033–1041

